The Journal of Immunology

The Orphan Immune Receptor LILRB3 Modulates Fc Receptor–Mediated Functions of Neutrophils

Yuxi Zhao, Esther van Woudenbergh, Jing Zhu, Albert J. R. Heck, Kok P. M. van Kessel, Carla J. C. de Haas, Piet C. Aerts, Jos A. G. van Strijp and Alex J. McCarthy

J Immunol 2020; 204:954-966; Prepublished online 8 January 2020;
doi: 10.4049/jimmunol.1900852
http://www.jimmunol.org/content/204/4/954

The Journal of Immunology is published twice each month by
The American Association of Immunologists, Inc.,
1451 Rockville Pike, Suite 650, Rockville, MD 20852

Print ISSN: 0022-1767 Online ISSN: 1550-6606.

The Orphan Immune Receptor LILRB3 Modulates Fc Receptor–Mediated Functions of Neutrophils

Yuxi Zhao,*,†,‡ Esther van Woudenbergh,* Jing Zhu,§,¶,‖,# Albert J. R. Heck,§,¶,‖,# Kok P. M. van Kessel,* Carla J. C. de Haas,* Piet C. Aerts,* Jos A. G. van Strijp,* and Alex J. McCarthy*,**

Neutrophils are critical to the generation of effective immune responses and for killing invading microbes. Paired immune receptors provide important mechanisms to modulate neutrophil activation thresholds and effector functions. Expression of the leukocyte Ig-like receptor (LILR)A6 (ILT8/CD85b) and LILRB3 (ILT5/CD85a) paired-receptor system on human neutrophils has remained unclear because of the lack of specific molecular tools. Additionally, there is little known of their possible functions in neutrophil biology. The objective of this study was to characterize expression of LILRA6/LILRB3 receptors during human neutrophil differentiation and activation, and to assess their roles in modulating Fc receptor–mediated effector functions. LILRB3, but not LILRA6, was detected in human neutrophil lysates following immunoprecipitation by mass spectrometry. We demonstrate high LILRB3 expression on the surface of resting neutrophils and release from the surface following neutrophil activation. Surface expression was recapitulated in a human PLB-985 cell model of neutrophil-like differentiation. Continuous ligation of LILRB3 inhibited key IgA-mediated effector functions, including production of reactive oxygen species, phagocytic uptake, and microbial killing. This suggests that LILRB3 provides an important checkpoint to control human neutrophil activation and their antimicrobial effector functions during resting and early-activation stages of the neutrophil life cycle. ***The Journal of Immunology*****, 2020, 204: 954–966.**

Neutrophils are armed with an arsenal of strategies to kill invading microbes and to orchestrate inflammation (1). Upon infection, neutrophils are immediately activated and recruited to the site of infection where they detect and kill microbes through exposure to reactive oxygen species (ROS) and/or antimicrobial compounds following phagocytosis or degranulation (2). Additionally, neutrophils modulate immune responses by releasing cytokine and lipid mediators. However, if neutrophils are mobilized at the wrong time or place, their potent effector functions and proinflammatory signals can damage the host and cause inappropriate inflammatory responses. Accordingly, neutrophils must be tightly regulated to avoid overreactive immune responses (3).

The activation threshold of neutrophils is tightly regulated to prevent inappropriate immune responses (4). Expression of inhibitory receptors and paired receptor systems provides major regulatory mechanisms (5, 6). However, although activation receptors including Fc receptors, G protein-couple receptors (GPCRs), and TLRs have been studied extensively, there remains poor knowledge of the role of inhibitory and paired receptors in the regulatory process.

Paired receptors systems describe families of membrane receptors that share very similar extracellular regions but differ in their transmembrane regions, cytoplasmic regions, and signaling capacity (6). Inhibitory receptors typically interact with self-proteins and provide mechanisms to raise activation thresholds and limit cell activity. Upon binding of ligands, ITIMs in the cytoplasmic tails of inhibitory receptors become phosphorylated, leading to docking of SH2 domain–containing tyrosine phosphatases and suppression of downstream signaling cascades (7). In disease situations, the ligands of inhibitory receptors are often downregulated or modified resulting in reduced inhibitory signals and a lowering of the activation threshold. Inhibitory receptors expressed on neutrophils include leukocyte-associated Ig-like

*Department of Medical Microbiology, University Medical Center Utrecht, Utrecht University, 3584 CX Utrecht, the Netherlands; †Institute for Immunology, School of Medicine, Tsinghua University, Beijing 100084, China; ‡School of Medicine, Tsinghua University, Beijing 100084, China; §Biomolecular Mass Spectrometry and Proteomics, University of Utrecht, 3584 CX Utrecht, the Netherlands; ¶Bijvoet Center for Biomolecular Research, University of Utrecht, 3584 CX Utrecht, the Netherlands; ‖Utrecht Institute for Pharmaceutical Sciences, University of Utrecht, 3584 CX Utrecht, the Netherlands; #Netherlands Proteomics Center, 3584 CX Utrecht, the Netherlands; and **MRC Centre for Molecular Bacteriology and Infection, Imperial College London, London SW7 2AZ, United Kingdom

ORCIDs: 0000-0002-4440-8257 (Y.Z.); 0000-0001-7363-6649 (E.v.W.); 0000-0001-8451-9173 (J.Z.); 0000-0002-2405-4404 (A.J.R.H.); 0000-0001-6253-0830 (J.A.G.v.S.); 0000-0002-4105-3737 (A.J.M.).

Received for publication July 19, 2019. Accepted for publication November 26, 2019.

This work was supported by the European Union's Horizon 2020 Research and Innovation Programme under Grant Agreement 700862. Y.Z. was supported by a grant from the program of China Scholarships Council (201406170045). J.Z. and A.J.R.H. acknowledge support from the Netherlands Organization for Scientific Research funding the Netherlands Proteomics Centre embedded in the roadmap facility *X-Omics* (Project 184.034.019). J.Z. additionally acknowledges support from the Chinese Scholarship Council.

The mass spectrometry data presented in this article have been submitted to the ProteomeXchange Consortium via the PRIDE partner repository under accession numbers PXD015561 and 10.6019/PXD015561.

Address correspondence and reprint requests to Dr. Alex J. McCarthy, MRC Centre for Molecular Bacteriology and Infection, Imperial College London, London SW7 2AZ, U.K. E-mail address: a.mccarthy@imperial.ac.uk

The online version of this article contains supplemental material.

Abbreviations used in this article: ATCC, American Type Culture Collection; DB, Dynabeads; HSA, human serum albumin; LAIR-1, leukocyte-associated Ig-like receptor 1; LILR, leukocyte Ig-like receptor; MOI, multiplicity of infection; MS, mass spectroscopy; β-*O*-GlcNAc, β-linked *N*-acetylglucosamine; pAb, polyclonal Ab; poly-RboP, polymer ribitol polyphosphate; rLILR, recombinant LILR; ROS, reactive oxygen species; Siglec-5, sialic acid–binding Ig-like lectin 5; SIRL-1, signal inhibitory receptor on leukocytes 1; SV, secretory vesicle; UMC, University Medical Center; VH, variable H chain; VL, variable L chain; WTA, wall teichoic acid.

receptor 1 (LAIR-1), signal inhibitory receptor on leukocytes 1 (SIRL-1), sialic acid–binding Ig-like lectin 5 (Siglec-5), and leukocyte Ig-like receptor (LILR)B2 (8–11). The ITIM signaling of these receptors can counteract activation of cells through ITAM signaling. Thus, inhibitory receptors can suppress Fc receptor–mediated activation including signals from FcγRIIA (CD32a) and the Fc common γ-chain cytoplasmic tail (used by FcγRIA or CD64 and FcαR or CD89) (4). Inhibitory receptors are often paired with activation receptor siblings that compete for the same ligands and regulate inhibitory signals (6). Siglec-14 possesses an almost identical ligand-binding domain to Siglec-5 but associates with ITAM-bearing DAP12 adaptor protein and can activate immune cells (12). LAIR-2 is released in a soluble form from neutrophils and can bind the same ligand as LAIR-1 but with a higher affinity, thereby providing a mechanism to reduce LAIR-1 inhibitory signals (13). Consequently, paired receptors modify activation thresholds and help to generate balanced immune responses.

LILRA6 (ILT8/CD85b) and LILRB3 (ILT5/CD85a) are paired receptors expressed by myelomonocytic leukocytes (3, 14). LILRA6 and LILRB3 have high similarity in their extracellular domain, and mAbs generated against these receptors bind to neutrophils. Yet, as the mAbs are cross-reactive, it has remained unclear which of these receptors is expressed in neutrophils and what their role is in neutrophil biology (5). LILRs are a family of 11 receptors with a powerful ability to modulate immune cell activity, function, and phenotype (15, 16). LILRA, including LILRA6, possess short cytoplasmic tails and signal through the ITAMs in the Fc common γ-chain. In contrast, LILRB, including LILRB3, possess long cytoplasmic tails containing their own ITIMs. Consequently, binding of ligands to LILRAs or LILRBs can enhance or lower the immune activation threshold. The best-characterized LILRs on neutrophils are LILRA2 and LILRB2, which are demonstrated to induce neutrophil activation upon recognition of microbially cleaved Igs (17) and to modulate neutrophil phagocytosis and degranulation (9), respectively. Additionally, the mouse ortholog paired-Ig-like receptor (PIR)–B regulates respiratory burst in neutrophils (18). Characterization of LILRA6 and LILRB3 in neutrophil biology has been hampered by a lack of LILRA6- and LILRB3-specific mAb and because native ligands are unknown.

Abs opsonize pathogens to enhance the capacity of phagocytic cells to detect and destroy pathogens (3). IgG and IgA are the dominant Ab isotypes in serum and are recognized by FcγRs or FcαR, respectively. Receptors expressed on neutrophils are FcγRI, FcγRIIIb, and FcαR that transduce signals through the ITAM of the receptor common γ-chain, as well as FcγRIIa and FcγRIIb that transduce signals through their own ITAM and ITIM domains, respectively (3). Inhibitory receptors, including LILRB1, LILRB2, and LILRB4 (19, 20), have been shown to inhibit IgG-mediated responses of phagocytes. Other inhibitory receptors, such as LAIR-1 and SIRL-1, inhibit IgA-mediated responses (21, 22). Although the established model of ITIM-mediated inhibition of ITAM-driven activation suggests inhibitory receptors modulate both IgG and IgA-mediated functions, confirmatory studies are required. Notably, no studies have assessed the role of LILR to modulate IgA-mediated responses of phagocytes.

In this study, we aimed to improve our understanding of LILRA6 and LILRB3 in neutrophil biology. We characterized their expression on resting neutrophils and during neutrophil activation. Next, we investigated their role in modulation of FcαR-mediated effector functions using mouse mAbs with cross-linking and agonistic properties as an LILR stimulant. However, as mouse IgG can bind and stimulate human FcγR (23), we additionally used a human FcγR inhibitor called FLIPr-like in our assays to ensure Fab, but not Fc, mediated Ab activation. This provided opportunities to probe LILR function and their capacity to modulate FcαR-mediated functions on neutrophils. We provide evidence that LILRB3 is expressed at the surface of resting and primed neutrophils, whereby it acts as a potent inhibitor of Fc receptor–mediated effector functions, including ROS production, phagocytosis, and killing of microbes. Expression can be recapitulated during differentiation of PLB-985 cells into neutrophil-like cells, providing a model to improve understanding of the molecular mechanisms of LILRB3. Our data demonstrate that LILRB3 might be considered as the target of therapeutics to modify neutrophil functions and immune responses during disease situations.

Materials and Methods

Expression of recombinant LILR and IgA1 mAb

Signal peptides and extracellular domains of LILR were amplified from cDNA vectors (Table I) and inserted into pcDNA3.4 vector. Forward primers contained an overhang for pcDNA3.4 vector, a BamHI restriction site, Kozak sequence, and LILR-specific region. Reverse primers contained an overhang for pcDNA3.4 vector, an NotI restriction site, stop codon, and polyhistidine tag. PCR amplifications were performed with Phusion High-Fidelity *Taq* Polymerase and thermocycling as follows: 1 cycle (98˚C for 2 min), 35 cycles (98˚C 15 s, 62˚C 30 s, and 72˚C 30 s), and 1 cycle (72˚C 10 min). Recombinant LILR (rLILR) was purified by affinity chromatography (ÄKTA pure; GE Healthcare Life Sciences) using nickel columns (GE Healthcare Life Sciences). Elutions were dialyzed into 50 mM Tris 300 mM NaCl (pH 8) at 4˚C.

Vectors encoding anti– wall teichoic acid (WTA)–4497-IgA1 or anti–human serum albumin (HSA)–GA645-IgA1 were constructed by cloning gBlocks containing human IgA1 H and L chain constant regions into pcDNA3.4 vectors. gBlocks containing variable H chain (VH) and variable L chain (VL) sequences were cloned into pcDNA3.4-HCIg-hG1 and pcDNA3.4-LCIg-hk, as well as upstream Kozak sequence and HAVT20 signal peptide, using NheI and BsiWI as the 3′ cloning sites for VH and VL, respectively, to preserve the Ig H and κ L chain amino acid sequence. VH and VL sequences were derived from previously described Abs directed against staphylococcal WTA GlcNAC-β (anti-WTA clone 4497; based on WO2014/193722) and against HSA (anti-HSA clone CA465) (24–26). Abs were expressed as IgG1/κ in EXPI293F cells (Life Technologies), essentially as described before (27), and purified by affinity chromatography (ÄKTA pure; GE Healthcare Life Sciences) using a protein A column (GE Healthcare Life Sciences). Elutions into 0.1 M citric acid (pH 3) were dialyzed against PBS at 4˚C.

rLILR and IgA1 were expressed in EXPI293F cells in EXPI media at 37˚C with 5% CO_2. Fifty micrograms of vector was packaged into 250 μg polyethylenimine MAX 40K (Polysciences) in 5 ml of Opti-MEM media (Life Technologies). After incubation at room temperature for 20 min, media was added to 50 ml of 2×10^6 cells/ml and cultured at 37˚C with 5% CO_2. Supernatants were harvested after 72 h of culture and dialyzed against 50 mM Tris 300 mM NaCl (pH 8).

Abs

The following unlabeled Abs were used in this study: anti-LILRA6 (clone 921330; R&D Biosystems), anti-LILRB1 (clone GHI/75; ITK Diagnostics), anti-LILRB3 (clone 222821; R&D Biosystems), anti-CD89 (clone MIPa; Bio-Rad Laboratories), mouse IgG1 isotype (SouthernBiotech), and mouse IgG2a isotype (SouthernBiotech). Abs conjugated with fluorescent labels used to measure receptor expression in this study are the following: anti-mouse IgG1-PE (Agilent Technologies), anti–CD35-PE (clone E11; BD Biosciences), anti–CD63-PE (clone 435; Immunotec), anti–CD11b-APC (BD Biosciences), anti–CD66b-FITC (BD Biosciences), anti–CD62L-PE (BD Biosciences), anti–CD63-FITC (Immunotec), anti–CD62L-FITC (BD Biosciences), anti–CD16-FITC (BD Biosciences), anti–CD32-FITC (BD Biosciences), anti–CD64-FITC (MIBI), anti–CD89-PE (Bio-Rad Laboratories), and anti–CD32-PE (Bio-Rad Laboratories). Hamster anti-mouse CD3e clone 145-2C11 (BD Biosciences) was used to test CD3ζ-mediated GFP expression in 2B4T cells. Abs used for Western blot assays were rabbit anti-LILRB3 polyclonal Abs (pAb) (Sino Biological), rabbit IgG, and goat anti-rabbit IgG-HRP (Abcam).

Neutrophil isolation and activation

This study was carried out in accordance with the recommendations of Medical Education and Training Center protocol 07-125/C and was approved on March 1, 2010, by the medical ethics committee of the University Medical Center (UMC) Utrecht with written informed consent from all subjects. All subjects gave written informed consent in accordance with the Declaration of Helsinki. The protocol was approved by the medical ethics committee of the UMC Utrecht. Neutrophils were isolated by Ficoll/Histopaque centrifugation as previously described and resuspended in RPMI 1640 supplemented with 0.05% HSA. Neutrophils were isolated with >98% purity and 99% viability. Secretory vesicle (SV) exocytosis was stimulated by incubation at 37˚C for 60 min. Priming was stimulated by incubation with 10 μg/ml TNF-α at 37˚C for 60 min. Granule exocytosis was stimulated by incubation with 1 μM fMLF and 10 μg/ml cytochalasin B for 60 min. In certain experiments, neutrophils were preincubated on ice with 5 μg/ml FLIPr-like to inhibit FcγR for 20 min (28).

Binding of mAb to Dynabeads or cells

Dynabeads (DB) or cells (35 μl of 5×10^6 cells/ml) were incubated with 5 μg/ml of mAb for 1 h at 4˚C. For detection of primary mAb, cells were incubated with 5 μg/ml of PE-conjugated goat anti-mouse IgG for 1 h at 4˚C. Fluorescence was measured by flow cytometry. DB or cells were gated based on forward- and side-scatter plots. To produce LILR-coated DB, C-terminal His-tagged rLILR were attached to Dynabeads His-Tag Isolation & Pulldown (Thermo Fisher Scientific).

Immunoprecipitation of LILRA6/B3

A total of 3×10^7 cells were washed in ice-cold PBS, pelleted, and lysed for 30 min at 4˚C using 500 μl of ice-cold 0.3% saponine-containing protease inhibitors 1:1000 4-(2-aminoethyl)benzenesulfonyl fluoride hydrochloride and leupeptin. After centrifugation for 15 min at 4˚C, 100 μl of supernatants were incubated at 4˚C with 25 μl of Dynabeads Protein A for immunoprecipitation (Thermo Fisher Scientific) for 2 h. DB had previously been coated with anti-LILRA6, anti-LILRB3 or isotype controls following standard protocol. DB were washed three times in ice-cold lysis buffer, resuspended in sample buffer, and heated to 95˚C for 5 min. DB lysates were separated by SDS-PAGE, blotted onto membranes, probed with rabbit anti-LILRB3 pAb or rabbit IgG, and detected with goat anti-rabbit HRP.

On-bead digestion of immunoprecipitated LILRA6/B3 and mass spectrometry analysis

DB for immunoprecipitation were washed three times in ice-cold ultrapure water, resuspended in 50 μl reduction buffer containing 2% (w/v) sodium deoxycholate, 200 mM Tris, and 10 mM tris(2-carboxyethyl)phosphine and heated in 95˚C for 10 min. Alkylation was done by adding 50 μl of 60 mM 2-chloroacetamide at room temperature. One microgram of chymotrypsin (Sigma-Aldrich) was added, and digestion was performed at 37˚C for 16 h. The supernatant was kept after centrifugation at 20,000 × *g* for 10 min at room temperature. Sodium deoxycholate was removed by acidic precipitation with 0.5% trifluoroacetic acid. Peptides were cleaned by Oasis PRiME HLB 96-well plates following manufacturer's instructions, dried by SpeedVac, and stored at −80˚C until mass spectroscopy (MS) analysis.

Peptides were separated and analyzed using an Agilent 1290 Infinity HPLC system (Agilent Technologies, Waldbronn, Germany) coupled online to a Q-Exactive Plus hybrid quadrupole-Orbitrap mass spectrometer (Thermo Fisher Scientific, Bremen, Germany). Reversed-phase separation was accomplished using a 100-μm inner diameter, 2-cm trap column (in-house, packed with ReproSil-Pur C18-AQ, 3 μm) (Dr. Maisch, Ammerbuch-Entringen, Germany) coupled to a 50-μm inner diameter, 50-cm analytical column (in-house, packed with Poroshell 120 EC-C18, 2.7 μm) (Agilent Technologies, Amstelveen, the Netherlands). Mobile-phase solvent A consisted of 0.1% formic acid in H_2O, and mobile-phase solvent B consisted of 0.1% formic acid in 80% acetonitrile. Trapping was performed at a flow rate of 5 μl/min for 5 min with 0% B, and peptides were eluted using a passive split flow of 300 nl/min for 80 min with 13–44% B over 65 min, 44–100% B over 3 min, 100% B for 1 min, 100–0% B over 1 min, and finally held at 0% B for 10 min. Mass spectra were collected in data-dependent acquisition mode, automatically switching between MS and MS/MS. Full scans (mass-to-charge ratio from 375 to 1600) were acquired at a resolution of 60,000 and a target of 3e6 ions or a maximum injection time of 20 ms. Fragmentation was induced for the top 15 peaks. Target peaks were isolated in a 1.4-Da isolation window and subjected to high-energy collision dissociation with a normalized collision energy value of 27%. MS/MS spectra (mass-to-charge from 200 to 2000) were acquired with a resolution of 30,000 using an automatic gain control setting of 1e5 ions or a maximum injection time of 50 ms. Charge-state screening was enabled, and precursors with unknown charge state or a charge state of 1 and >6 were excluded.

Raw shotgun liquid chromatography MS/MS data were searched with Proteome Discoverer (version 2.2; Thermo Fisher Scientific) using the Mascot search engine (version 2.6.1). Processing nodes included spectrum file reader, Minora Feature Detector (for label-free quantification), spectrum selector, Mascot, and Percolator. Mascot searches were performed against a combined database of UniProt Swiss-Prot database: *Homo sapiens* (canonical and isoform) (September 2019, 20,417 entries) and manually checked variants of LILRA6/B3 (September 2019, 29 entries). Searches were performed with fixed Cys carbamidomethylation and variable Met oxidation and Ser/Thr phosphorylation of peptides. Chymotrypsin was chosen for cleavage specificity with a maximum of two missed cleavages allowed. The searches were performed using a precursor mass tolerance of 10 ppm and a fragment mass tolerance of 0.05 Da (high-energy collision dissociation), followed by data filtering using Percolator, resulting in 1% false discovery rate. Mascot scores >20 were accepted. The mass spectrometry data have been deposited to the ProteomeXchange Consortium via the PRIDE partner repository with the dataset identifier PXD015561 and 10.6019/PXD015561 with the following login information: username: reviewer73469@ebi.ac.uk; password: spzXpdnf.

Detection of LILRB3 in cell supernatants

A total of 3×10^7 cells were pelleted. Supernatants were concentrated 10 times on a 3-kDa ultra centrifugal filter column (Amicon). Supernatants were mixed 1:1 with 2× sample buffer, incubated at 95˚C for 10 min, separated by SDS-PAGE, and blotted onto membranes. After blocking, membranes were washed, probed with 1:5000 rabbit anti-LILRB3 pAb or rabbit IgG control, washed, and probed with 1:10,000 goat anti-rabbit IgG-HRP.

Culture and differentiation of PLB-985 cells

PLB-985 cells were cultured in RPMI 1640 supplemented with 10% FCS at 37˚C with 5% CO_2. To differentiate toward a neutrophil-like phenotype, PLB-985 cells were seeded at a density of 1×10^5 cells/ml and cultured in the presence of 1.25% DMSO for up to 5 d (23, 29). To lyse DMSO-differentiated PLB-985 cells, 1×10^7 cells were washed in ice-cold PBS, pelleted, and lysed for 30 min at 4˚C using 500 μl of ice-cold 0.3% saponine-containing protease inhibitors 1:1000 4-(2-aminoethyl) benzenesulfonyl fluoride hydrochloride and leupeptin. Immunoprecipitation of LILRB3 from PLB-985 cell lysates, and subsequent detection of LILRB3, was performed using the same methodologies as for neutrophils.

Construction of LILR reporter 2B4T cells

The 2B4 NFAT-GFP T cell reporter cells contain a NFAT-GFP construct composed of three tandem NFAT-binding sites fused with enhanced GFP cDNA (30). To express fusion proteins, DNA fragments containing the coding domain sequence of the extracellular and transmembrane domains of LILRA6 and LILRB3 and the CD3ζ cytoplasmic tail were synthesized by Integrated DNA Technologies and were ligated into a dual promoter lentiviral vector (BIC-PGK-Zeo-T2a-mAmetrine; RP172 derived from no.2025.pCCLsin.PPT.pA.CTE.4·-scrT.eGFP.mCMV.hPGK.NG-FR.pre, as previously described) via Gibson reaction (31). Vectors containing correct inserts were confirmed by sequencing. The RP172 vector contains human EF1A promoter for potent expression of the cloned downstream gene and the selection marker for zeocin resistance. Lentiviral particles were created in HEK293T cells that were seeded at 6.25×10^4 cells/ml in RMPI 1640 with 10% FCS, 100 μg/ml penicillin, and 100 μg/ml streptomycin and cultured at 37˚C with 5% CO_2 for 24 h. Fifty microliters of RMPI 1640 and TransIT-LT1 Transfection Reagent (Mirus Bio) were mixed and incubated for 5 min at room temperature. Subsequently, 0.25 μg packaging mixture (containing equal parts of pVSV-G, pMDL, and pRSV vectors) and 0.25 μg of RP172 vector were added, mixed, and incubated at room temperature for 20 min. This mixture was added to 1 ml of HEK293T cells and incubated at 37˚C and 5% CO_2 for 72 h. One hundred microliters of the supernatant containing lentivirus particles was added to 500 μl of 1×10^5 cells/ml of 2B4T cells in RPMI 1640 supplemented with 10% FCS with 100 μg/ml penicillin, 100 μg/ml streptomycin, and 8 μg/ml polybrene. After centrifugation at 2000 rpm for 90 min at 33˚C, cells were supplemented with 500 μl of RPMI 1640 containing 10% FCS with 100 μg/ml penicillin and 100 μg/ml streptomycin and incubated at 37˚C

with 5% CO_2. After 72 h, cells were supplemented with an 5 ml of RPMI 1640 containing 10% FCS, 100 μg/ml penicillin, 100 μg/ml streptomycin, and 400 μg/ml zeocin to select for transfectants for 14 d. Cell cultures were formed, and LILR expression was measured using anti-LILR mAb and flow cytometry analysis.

Induction of GFP expression in LILRCD3ζ reporter 2B4T cells

Ninety-six-well plates were coated at 4˚C overnight with 40 μl of 15 μg/ml anti-CD3ζ, anti-LILRA6, anti-LILRB3, or respective isotype control mAbs diluted in $NaHCO_3$ buffer. Two hundred microliters of 2B4T cells were seeded in 96-well plates at 2.5×10^5 cells/ml in RPMI 1640 containing 10% FCS, 100 μg/ml penicillin, and 100 μg/ml streptomycin and cultured at 37˚C with 5% CO_2. After 18 h, cells were resuspended in PBS, and their fluorescence was measured by flow cytometry.

Measurement of neutrophil activation

White 96-well plates were coated at 4˚C overnight with 40 μl of 5 μg/ml anti-CD89, anti-LILRB3, anti-LILRA6, mouse IgG1 isotype, or mouse IgG2a isotype diluted in $NaHCO_3$ buffer. Neutrophils were resuspended in IMDM with 0.05% HSA to 2.5×10^6 cells/ml. Fifty microliters of neutrophils were incubated on wells. After incubation at room temperature for 30 min, 100 μl of prewarmed luminol balanced salt solution (final concentration of luminol 220 μM) was added to wells after washing. The level of ROS production was determined as area under the curve, with background subtraction of neutrophils only, during 60 min.

Assessing modulation of IgA-mediated neutrophil activation

Clear 96-well plates were coated at 4˚C overnight with 40 μl of 5 μg/ml anti-LILRA6 or mouse IgG1 isotype diluted in $NaHCO_3$ buffer. Neutrophils were resuspended in IMDM with 0.05% HSA to 2.5×10^6 cells/ml. Fifty microliters of neutrophils were incubated on wells coated with anti-LILRA6, anti-LILRB3, mouse IgG1, or IgG2a mAb for 60 min at room temperature. After resuspension, neutrophils were transferred to wells of white plates that contained 100 μl of luminol balanced salt solution to measure luminescence. These wells had previously been coated with anti-CD89 or mouse IgG1 isotype control (40 μl of 5 μg/ml, incubated at 4˚C overnight). The production of ROS was measured via luminescence detection at 2-min intervals. The level of ROS production was determined as area under the curve, with background subtraction of neutrophils only, during 60 min.

IgA-mediated phagocytosis

Dynabeads M 280 Streptavidin (Thermo Fisher Scientific), which have a 2.8-μm diameter, were FITC labeled by incubation for 30 min in 500 μg/ml FITC. After washing, DB were coated with biotinylated HSA (100 μg/ml) following standard protocol. DB were opsonized with anti–HSA-IgA1 or anti–WTA-IgA1 by incubation for 30 min at room temperature. Bound IgA was detected using 0.3 μg/ml anti–IgA-AF647 and flow cytometry. To measure phagocytic uptake, DB were mixed at an multiplicity of infection (MOI) of 10:1 with 40 μl of 2.5×10^6 neutrophils/ml and incubated for 30 min at 37˚C with 200 rpm. Neutrophils were washed and fixed in 1% paraformaldehyde. Fluorescence of neutrophils was measured by flow cytometry, and the percentage of FITC-positive neutrophils was measured. In both ROS production and phagocytosis experiments, neutrophils were preincubated for 60 min at 37˚C with 5% CO_2 on 96-well plates coated at 4˚C overnight with anti-LILRA6 or mouse IgG1 isotype mAb.

IgA-mediated phagocytosis and killing of Staphylococcus capitis

S. capitis American Type Culture Collection (ATCC) 28740 and ATCC 28740-H strains were cultured in Tryptic Soy Broth (supplemented with 10 mg/ml chloramphenicol if required) at 37˚C until absorbance at OD_{600} = 0.4. The *S. capitis* ATCC 29740-H strain carries the plasmid pRB474-*tarFI*$_2$*J*$_2$*L*$_2$*S*, which encodes the operon required for expression of polymer ribitol polyphosphate (poly-RboP) WTA backbone with β-linked *N*-acetylglucosamine (β-*O*-GlcNAc) modifications (32). Thus, ATCC 29740-H is a hybrid strain expressing native WTA (poly-glycerophosphate with α-*O*-*N*-acetylgalactosamine modifications) and foreign WTA (poly-RboP and β-*O*-GlcNAc modifications). Bacteria were incubated with IgA1 mAb for 30 min on ice. Anti–human IgA–AF648 and flow cytometric analysis were used to detect surface bound IgA1. To FITC-labelled *S. capitis*, midlogarithmic phase cultures were incubated in 10 mg/ml FITC for 30 min on ice and washed five times in PBS with 0.1% BSA. To assess IgA-dependent phagocytic uptake, FITC-labeled bacteria (5 μl of 3×10^8 CFU/ml) and neutrophils (45 μl of 3×10^6 cells/ml) were mixed at an MOI of 10:1, were centrifuged at $500 \times g$ for 3 min to initiate the assay, and were incubated for 30 min at 37˚C with 5% CO_2 with 200 rpm. After washing, fluorescence of neutrophils was measured by flow cytometry.

To measure killing, bacteria (5 μl of 1×10^8 CFU/ml) and neutrophils (45 μl of 1×10^7 cells/ml) were mixed at an MOI of 1:1 and incubated for 60 min at 37˚C with 5% CO_2. Reactions were stopped by addition of 200 μl of 0.3% ice-cold saponine and incubation on ice for 15 min. CFU per milliliter were enumerated by serial dilution and culture of Brain Heart Infusion Agar Plates. All assays were performed in RPMI 1640 supplemented with 0.05% heat-inactivated human pooled serum. In both phagocytosis and killing experiments, neutrophils were preincubated for 60 min at 37˚C on 96-well plates previously coated at 4˚C overnight with anti-LILRA6 or mouse IgG1 isotype mAb. Datasets were tested for normal distributions using Shapiro–Wilk normality test and analyzed using parametric or nonparametric approaches as described in figure legends.

Results

LILRB3 is expressed by human neutrophils

We first assessed anti-LILRA6 and anti-LILRB3 mAb cross-reactivity. Recombinant extracellular domains of LILA6, -B1, and -B3 were expressed in a eukaryotic expression system. Both anti-LILRA6 and anti-LILRB3 bound to rLILRA6- and rLILRB3-, but not rLILRB1-, coated magnetic beads (Fig. 1A, 1B). This indicated anti-LILRA6 and anti-LILRB3 are cross-reactive. Anti-LILRA6 bound better to rLILRA6, and anti-LILRB3 had enhanced binding to rLILRB3. This could be due to differences in affinity or glycosylation.

Table I. LILR cDNA vectors and cloning vectors

cDNA vector	Primers
LILRA6	Forward
RDC0458 (R&D Systems)	5′-CTCTAGAGGATCGAACCCTTGGATCCACCACCATGACCCCCACCCTCGCAGCCCTGCTCTGCCT-AGGGCTGAGTCTGGGCCCCAGG-3′
	Reverse
	5′-CTAACCGGTAGGGATCGAACCCTTGCGGCCGCCTAGTGGTGATGGTGGTGATGGCGGATGAG-ATTCTCCACTGTG-3′
LILRB3	Forward
HG11978-M (Sino Biological)	5′-CTCTAGAGGATCGAACCCTTGGATCCACCACCATGACGCCCGCCCTCACAGCCCTGCTCTGCC-TTGGGCTGAGTCTGGGCCCCAGGA-3′
	Reverse
	5′-CTAACCGGTAGGGATCGAACCCTTGCGGCCGCCTAGTGGTGATGGTGGTGATGCTCCAGGTAT-CTTCCCAGACCAGG-3′
LILRB1	Forward
ORF005932 (abmgood)	5′-CTCTAGAGGATCGAACCCTTGGATCCACCACCATGACCCCCATCCTCACGGTCCTG-3′
	Reverse
	5′-CTAACCGGTAGGGATCGAACCCTTGCGGCCGCCTAGTGGTGATGGTGGTGATGCGACCCAGT-GGGGGTGAGGGGC-3′

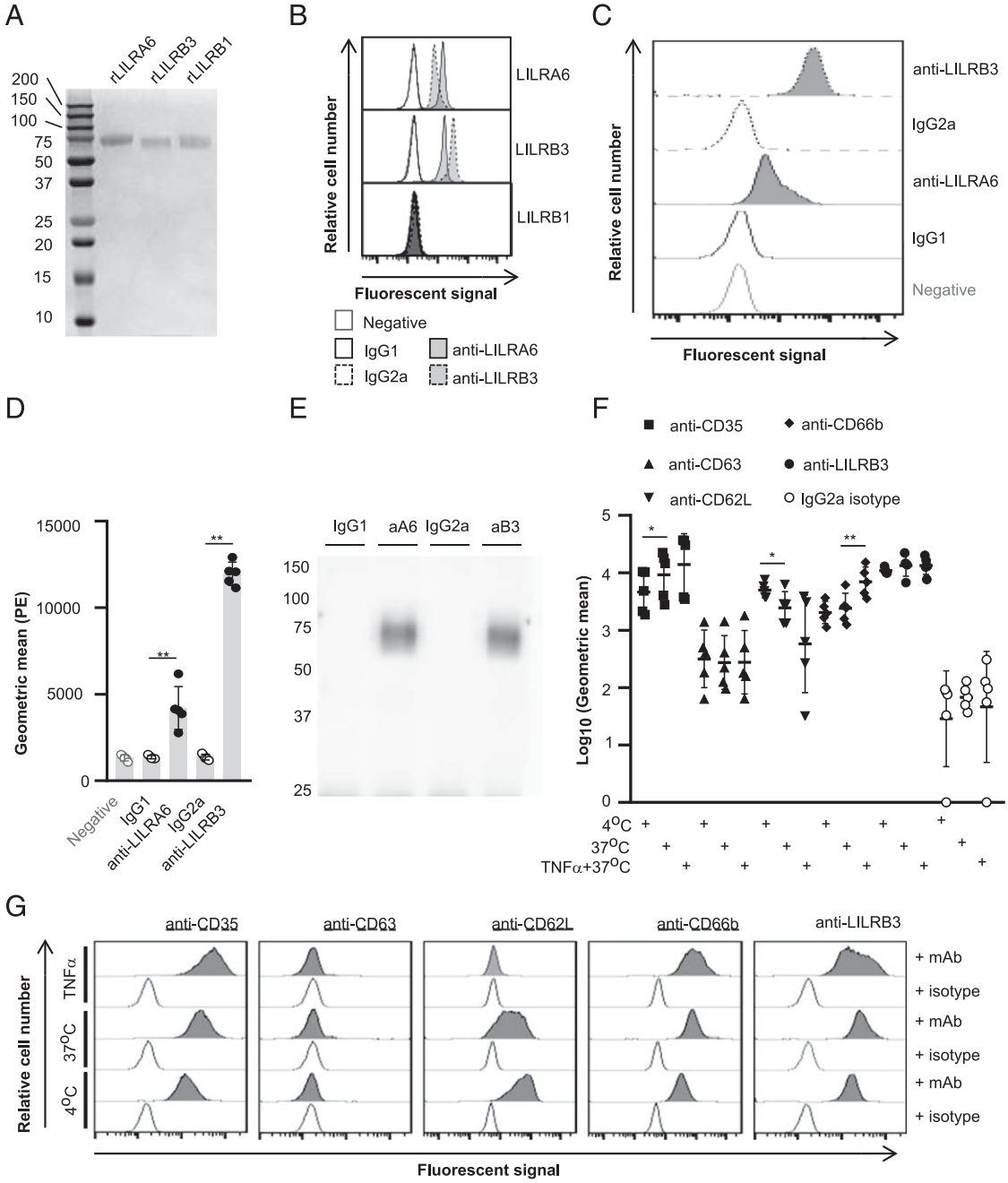

FIGURE 1. LILRB3 is expressed on the surface of resting neutrophils and is downregulated upon priming. (**A**) Separation of rLILRA6, LILRB3, and LILRB1 purified from eukaryotic expression system by SDS-PAGE. (**B**) Binding of anti-LILRA6, anti-LILRB3, and isotype control mAb to DB coated with rLILR. Representative flow cytometry plots of $n = 3$ are shown. (**C** and **D**) Binding of anti-LILRA6, anti-LILRB3, and isotype control mAb to resting neutrophils, using anti-IgG-PE as a secondary mAb. A representative experiment (C) and the integrated results from five separate experiments (D) were compared by Student *t* test. (**E**) Immunoprecipitation of LILRA6 and/or LILRB3 from the surface of resting neutrophils. Neutrophil lysates were incubated with 5 μg/ml anti-LILRA6 (aA6), anti-LILRB3 (aB3), IgG1 or IgG2a, and DB protein G. Immunoprecipitated proteins were eluted from beads, separated via SDS-PAGE, blotted onto membranes, and detected using rabbit anti-LILRB3 pAb or rabbit IgG and goat anti-rabbit IgG-HRP. Data are representative of $n = 3$ independent experiments. (**F** and **G**) Priming of neutrophils with TNF-α does not alter LILRB3 expression levels. Neutrophils were incubated at 4˚C (resting), at 37˚C (SVs exocytosed), or 37˚C in the presence 5 μg/ml TNF-α (primary granules exocytosed). Anti–IgG-PE used as a secondary mAb for anti-LILRB3 and IgG2a isotype control. Integrated results from five separate experiments (F) were compared by Student *t* test. Data from a representative experiment are shown (G). $*p < 0.05$, $**p < 0.01$.

Next, we investigated LILRA6 and LILRB3 expression on primary neutrophils. Data from five healthy human donors were analyzed as geometric mean fluorescence in comparison with neutrophils stained with isotype control mAbs. Average geometric mean was 4729 and 1415 for anti-LILRA6 versus IgG1 isotype ($p < 0.01$) and 12,190 versus 1459 for anti-LILRB3 and IgG2a isotype ($p < 0.01$) (Fig. 1C, 1D). LILRA6 (50 kDa) and LILRB3 (66.9 kDa) can be discriminated based on size because of differences in the length of their cytoplasmic tails. We immunoprecipitated receptors using neutrophil lysates in combination with anti-LILRA6, anti-LILRB3, or isotype control mAb and protein G–coated beads. Immunoprecipitated proteins were separated by SDS-PAGE and blotted onto membranes. Using anti-LILRB3 pAb for probing, a single protein band of around 75 kDa was detected

after immunoprecipitation with anti-LILRA6 and anti-LILRB3 (Fig. 1E). As a control, we confirmed that anti-LILRB3 pAb was able to detect both rLILRA6 and rLILRB3 by Western blotting (Supplemental Fig. 1A). Collectively, the data suggested that one receptor, most likely LILRB3, was expressed on neutrophils at detectable levels. To confirm the identity of the protein, we performed mass spectrometry analysis of immunoprecipitated proteins from neutrophils lysates. A total of 21 LILRA6 or LILRB3 peptides were detected in samples immunoprecipitated using anti-LILRA6 and anti-LILRB3 mAb, which were absent in samples immunoprecipitated using control anti-IgG1 and anti-IgG2a mAb. Alignment of peptide sequences of all full-length LILRA6 and LILRB3 sequences in the UniProt database revealed 0 and 7 peptides were LILRA6- and LILRB3-specific, respectively. Notably, peptides 5 (QRPAGAAETEPKDRGLL) and 6 (RRSSPAADVQEENLY) mapped to the cytoplasmic ITIM domain of LILRB3 and were found in samples from all five donors (Supplemental Fig. 1B, Table II). Therefore, mass spectrometry analysis indicated that neutrophils from 5/5 donors expressed LILRB3, and 0/5 donors expressed LILRA6. This is consistent with previous proteomic analysis revealing LILRB3 to be a major constituent of secretory granules (SVs) (33).

Immune receptors can also be expressed in SVs or granules. We compared LILRB3 expression between resting neutrophils and those incubated at 37˚C, which is enough to mobilize SV release (34). Incubation at 37˚C induced upregulation of SV marker CD35, but not granule marker CD63 (Fig. 1F, 1G). Additionally, CD62L was downregulated. There was no significant change in LILRB3 expression (Fig. 1G). Incubating neutrophils with 5 μg/ml TNF-α induced upregulation of gelatinase granule marker CD66b, but no significant up- or downregulation of CD63, CD35, or CD62L (Fig. 1F, 1G). Mean LILRB3 surface content did not change upon TNF-α priming. Individual flow cytometry plots suggested LILRB3 levels were more heterogenous following TNF-α priming (Fig. 1G). This could mean LILRB3 is differentially regulated in subpopulations. Alternatively, there could have been simultaneous up- and downregulation through TNF-α priming–associated mechanisms.

PLB-985 cell differentiation toward a neutrophil-like phenotype is associated with LILRB3 upregulation

The expression of LILRB3 on the surface of resting neutrophils suggests LILRB3 may function during neutrophil differentiation. Recently, upregulation of LILRA6/B3 transcripts was reported during differentiation of the promyeloid tumor cell line PLB-985 toward a neutrophil-like phenotype (29). We examined LILRA6/B3 expression during neutrophil-like differentiation of PLB-985 cells. Undifferentiated PLB-985 cells expressed CD32 and CD89, but not CD16 or CD11b, as reported (Fig. 2A) (21, 29). Fluorescence of undifferentiated PLB-985 cells was elevated for anti-LILRB3 compared with IgG2a isotype (Fig. 2A, Supplemental Fig. 2A), suggestive that LILRA6/B3 are expressed at low basal levels on undifferentiated PLB-985 cells.

Culture of PLB-985 cells with 1.25% DMSO for 5 d led to increased CD89 and CD11b surface expression (Supplemental Fig. 2B), which was consistent with previous reports of neutrophil-like differentiation (22). LILRA6/B3 was upregulated during differentiation with 1.25% DMSO (Fig. 2B, 2C), and after 5 d of differentiation, there was a 2.54 ± 0.3–fold upregulation. This was concomitant with upregulation of CD89 and CD62L (Fig. 2D).

To confirm expression of LILRA6 and/or LILRB3 in PLB-985 cells, we probed proteins immunoprecipitated from DMSO-differentiated PLB-985 cells by Western blot. Using rabbit anti-LILRB3 pAb for secondary detection, we found the presence of a single band at 75 kDa, most likely LILRB3, following immunoprecipitation with

Table II. Mass spectrometry detection of LILRA6 and LILRB3 in neutrophil lysates following immunoprecipitation

Peptide	Donor 1		Donor 2		Donor 3		Donor 4		Donor 5	
	Anti-A6	Anti-B3	Anti-A6	Anti-B3	Anti-A6	Anti-B3	Anti-A6	Anti-B3	Anti-A6	Anti-B3
1			7.45×10^6	1.13×10^6						
2			3.39×10^7	7.79×10^6						
3			5.09×10^7	1.12×10^7						
4			1.70×10^6	4.28×10^5						
5	7.17×10^6	3.65×10^6	1.04×10^7	1.15×10^7	3.03×10^7	5.39×10^7	2.36×10^7	6.10×10^7	7.70×10^7	1.82×10^7
6	3.42×10^5		1.55×10^6		3.09×10^6	1.89×10^6	2.34×10^6	6.23×10^6	1.17×10^7	1.40×10^6
7			4.27×10^7	1.14×10^7						

Peptide sequences are as follows: 1) QCGSDVGYNRF, 2) TLQCGSDVGYNRF, 3) DSQQLHSRGF, 4) SSAGWSEPSDPLEMVMTGAY, 5) QRPAGAAETEPKDRGLL, 6) RRSSPAADVQEENLY, and 7) RLHKEGSPEPL.

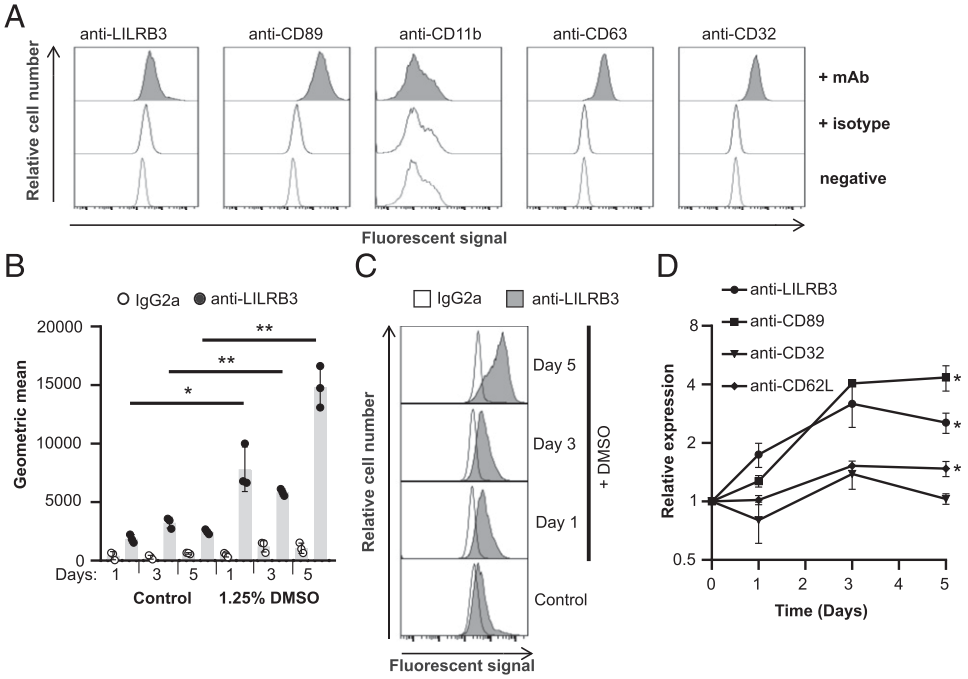

FIGURE 2. Differentiation of neutrophil-like PLB-985 cells is associated with enhanced LILRA6/B3 surface expression. (**A**) Undifferentiated PLB-985 cells express low levels of LILRA6/B3. PLB-985 cells were cultured in RPMI 1640 at 37˚C with 5% CO_2 and stained with primary Abs. Anti–IgG-PE was used as a secondary mAb for anti-LILRB3 and IgG2a isotype control. A representative experiment from three sperate experiments is shown. (**B**–**D**) DMSO-differentiated PLB-985 cells expressed enhanced surface levels of LILRA6/B3. PLB-985 cells were cultured in the presence or absence of 1.25% DMSO at 37˚C with 5% CO_2 for up to 5 d. Cells were stained with mAb, and fluorescence was measured by flow cytometry. Integrated results from three separate experiments (B) were compared by Student *t* test. Data from a representative experiment are shown (C). Relative receptor expression on DMSO-differentiated PLB-985 populations to undifferentiated PLB-985 populations (D) was plotted, in which Student *t* test was used to compare the relative receptor expression between day 0 and day 5. $*p < 0.05$, $**p < 0.01$.

anti-LILRA6 and anti-LILRB3 mAb, but not respective isotype controls. We believe that the secondary Ab detected L chain Ig and IgH at band sizes 25 and 50 kDa, respectively. Thus, LILRB3 expression was upregulated in PLB-985 cells cultured in the presence of 1.25% DMSO in comparison with control cells.

LILRB3 is downregulated upon neutrophil activation

As mature neutrophils alter the composition of their surface receptors upon exposure to environmental stimuli, we next investigated the surface expression of LILRB3 during neutrophil activation. Fluorescence of neutrophils incubated at 37˚C or 37˚C in the presence of fMLF and cytochalasin B was normalized to fluorescence of neutrophils incubated at 4˚C. Incubation at 37˚C with fMLF and cytochalasin B led to CD63 upregulation, CD35 downregulation, CD66b upregulation, and CD62L downregulation (Fig. 3A, 3B), which are typical markers of neutrophil degranulation. Degranulation was associated with LILRB3 downregulation ($\log_{10}$ geometric mean 4.12 ± 0.18 versus 3.16 ± 0.45, $n = 5$, $p < 0.05$). In addition, soluble LILRB3 was detected in supernatants of neutrophils incubated with fMLF and cytochalasin B, but not buffer control (Fig. 3C).

Proteases contained in granules can cleave immune receptors, including CD62L, from the cell surface upon degranulation. To understand whether proteases released during degranulation cleaved LILRB3 from the neutrophil surface, we compared receptor expression on neutrophils incubated in the supernatant of previously degranulated neutrophils or a buffer control. Flow cytometry revealed no change in CD63 expression, indicating that the supernatant of degranulated neutrophils alone did not induce degranulation of resting neutrophils (Fig. 3D, 3E). The supernatant of degranulated neutrophils, but not buffer, induced downregulation of CD62L. This indicated that proteases in the supernatant were active. However, LILRB3 was not downregulated, indicating that proteases contained within granules were not enough to release soluble LILRB3 (Fig. 3D, 3E).

Ligation of LILRB3 does not activate neutrophils

Inhibitory receptors can modify activation thresholds. The 2B4 NFAT-GFP reporter cells expressing chimeric proteins, consisting of extracellular and transmembrane domains of immune receptors fused to the CD3ζ cytoplasmic tail, have been used to identify agonists of immune receptors, including LAIR-1 and LILR (35, 36). We developed 2B4T NFAT-GFP reporter cells to identify ligands that could efficiently cross-link LILRA6 and/or LILRB3 (Supplemental Fig. 3A). Surface expression of chimeric proteins, composed of LILR extracellular and transmembrane domains fused to the CD3ζ cytoplasmic tail containing 3× ITAM motifs, was detected in transduced cells (Supplemental Fig. 3B). GFP expression was induced in 2B4T cell populations by stimulating native CD3 with anti-CD3 mAb (Supplemental Fig. 3C, 3D). Next, we tested agonistic effects of anti-LILR mAb (Fig. 4A, 4B). After incubation on anti-LILRA6 mAb–coated wells, significantly more LILRA6CD3ζ-expressing 2B4T cells were GFP positive compared with control 2B4T cells. Likewise, anti-LILRB3 induced GFP production in a larger proportion of LILRB3CD3ζ-expressing 2B4T cells compared with control cells. Both anti-LILRA6 and anti-LILRB3 activated both LILRA6 and LILRB3 fusion proteins (Fig. 4A), indicating agonistic effects are cross-reactive. Notably, anti-LILRA6 was a better agonist of both receptors than anti-LILRB3. Differences in agonistic properties could be due to mAb-target affinities or glycosylation.

Neutrophils produce significant levels of ROS by cross-linking activation receptors including CD32 (FcγR2A), CD89 (FcαR), or LILRA2. We tested whether continuous ligation of LILRB3 could induce neutrophil activation and ROS production. Exposure of

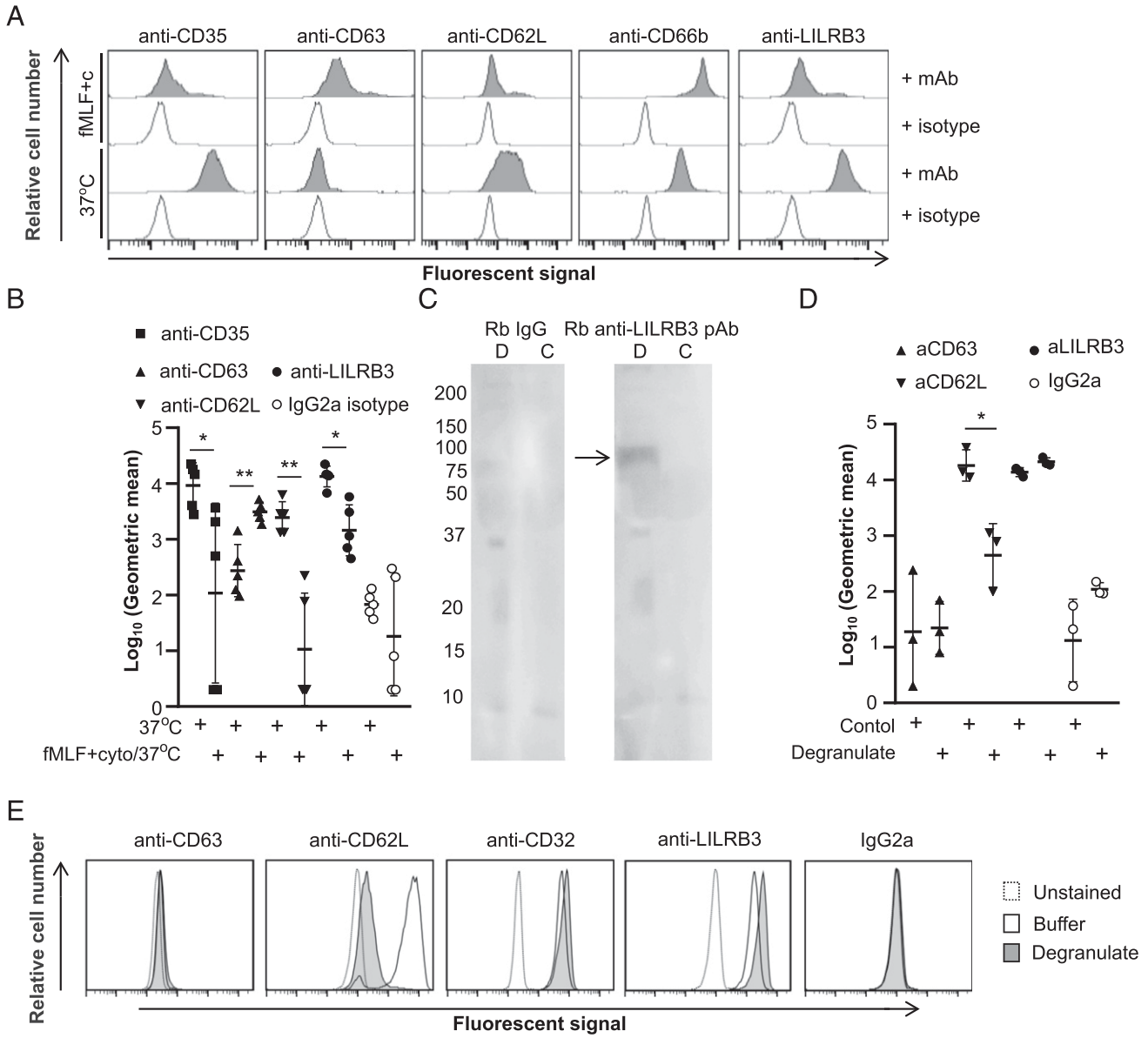

FIGURE 3. Neutrophil activation is associated with downregulation of LILRB3 from the surface. (**A** and **B**) Degranulation of neutrophils induced downregulation of surface LILRB3 expression levels. Neutrophils were incubated at 37˚C (SVs exocytosed) or 37˚C in the presence of fMLF and cytochalasin B (granules exocytosed) and then stained for receptor expression. Anti–IgG-PE was used as a secondary mAb for anti-LILRB3 and IgG2a isotype control. A representative experiment (A) and the integrated results from five separate experiments (B) are shown. The mean fluorescence intensity of neutrophil populations was normalized against unstained control neutrophils within each condition. Background level of receptor expression on neutrophils incubated at 37˚C was normalized to 1 (37/37˚C). Relative surface expression of receptors was calculated at 37˚C in presence of fMLF and cytochalasin B in comparison with 37˚C for granule release. (**C**) LILRB3 is detected in the supernatant of degranulated neutrophils. Supernates representing neutrophils degranulate (**D**) (incubation in presence of fMLF and cytochalasin B at 37˚C) or buffer control (C) (incubation in 37˚C) were separated by SDS-PAGE, blotted onto membranes, and probed with rabbit anti-LILRB3 pAb or rabbit IgG and detected using goat anti-rabbit IgG-HRP. Data representative of $n = 3$. (D and **E**) Proteases in neutrophil degranulate are not sufficient to induce downregulation of surface LILRB3 expression. Neutrophils were incubated in the supernatant of previously degranulated neutrophils or control buffer for 1 h at 37˚C and were then stained for receptor expression. Anti–IgG-PE used as a secondary mAb for anti-LILRB3 and IgG2a isotype control. Integrated results from three separate experiments (D) compared $\log_{10}$ (geometric mean fluorescence) values between neutrophils incubated at 37˚C in degranulate or control buffer by Student t test. Representative flow cytometry plots are shown (E). $^*p < 0.05$, $^{**}p < 0.01$.

neutrophils to anti-CD89 mAb led to increased luminescent signals and ROS production (Fig. 4C). Incubation of neutrophils on anti-LILRA6– or anti-LILRB3–coated wells did not induce enhanced luminescence signals (Fig. 4C). Data were consistent for neutrophils from five donors, indicative that LILRB3 cross-linking does not activate ROS production.

LILRB3 inhibits Fc receptor–mediation activation

We aimed to test whether LILRB3 could modulate Fc receptor–mediated ROS production using anti-LILRA6 and anti-LILRB3 mAb. Exposure of neutrophils to mouse IgG1- or IgG2a-coated wells induced significant luminescence signals (Supplemental Fig. 4A). This is likely induced through cross-linking of human FcγR via the Fc region of mouse IgG. Neutrophils exposed to anti-LILRA6 IgG1, which is an agonist of LILRB3, produced significantly lower luminescent signals compared with neutrophils exposed to control IgG1 mAb (Supplemental Fig. 4B, 4C). Anti-LILRA6 treatment induced a 4.54-fold downregulation of IgG1-mediated ROS production across donors, implying LILRB3 cross-linking suppresses FcγR-mediated activation.

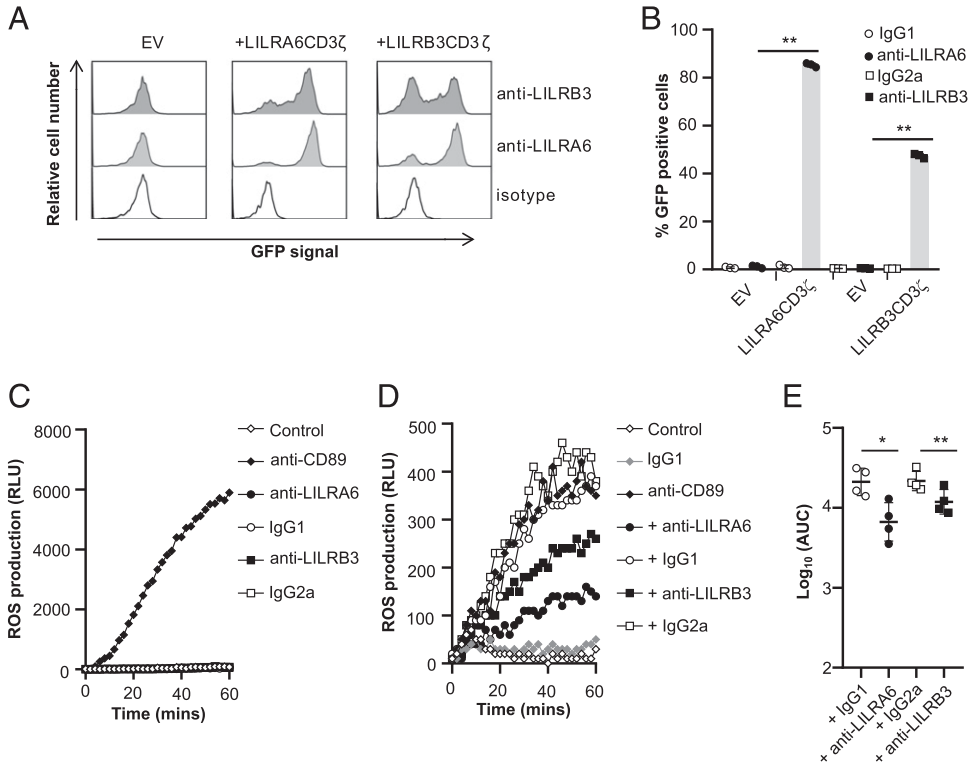

FIGURE 4. Cross-linking of LILRB3 suppresses FcαR-mediated activation. (**A** and **B**) GFP expression in 2B4T cells expressing LILRCD3ζ (A6 and B3) fusion proteins or empty vector (EV) control 2B4T cells following incubation at 37˚C. Plates were previously coated with anti-LILRA6, anti-LILRB3, or isotype mAb. These mAb served as the agonist in these assays. Cells were incubated in coated wells for 18 h, and GFP expression was measured by flow cytometry analysis. A representative experiment (A) and the integrated results from three separate experiments (B) were compared by Student *t* test. $*p < 0.05$, $**p < 0.01$. (**C**) Cross-linking of LILRB3 does not induce ROS production by neutrophils. Neutrophils were incubated in the presence of 5 μg/ml FLIPr-like for 20 min and then incubated on plates containing luminol. Plates were previously coated with anti-CD89, anti-LILRA6, anti-LILRB3, or isotype mAb. These mAb served as the agonist in these assays, and relative luminescence unit (RLU) was measured over 60 min as an indicator of ROS production. (**D** and **E**) Cross-linking of LILRB3 suppresses CD89-mediated ROS production by neutrophils. Neutrophils ($n = 4$) were incubated on plates previously coated with anti-LILRA6, anti-LILRB3, or IgG1 or IgG2a mAb. After 1 h, neutrophils were stimulated through FcαR/CD89 by incubation on plates containing luminol that were previously coated with anti-CD89 or IgG1 isotype control. RLU was measured over 60 min as an indicator of ROS production. A representative experiment (D) and the integrated results from four separate experiments (E) were compared by Student *t* test. $*p < 0.05$, $**p < 0.01$.

Next, we investigated whether LILRB3 could modulate the activation of neutrophils through FcαR. To minimize mouse IgG background activation of human FcγR, we pretreated neutrophils with FLIPr-like, which can bind human FcγR and inhibit interactions with IgG (29). This ensured cross-linking of receptors (CD89 and LILRB3) via Fab regions of mAb while limiting cross-linking of FcγR via Fc regions of mAb. Indeed, FLIPr-like inhibited activation of neutrophils via mouse IgG1 and IgG2a (Supplemental Fig. 4A). Furthermore, ROS production induced by anti-CD89 mAb was reduced in the presence of FLIPr-like (Supplemental Fig. 4D).

There was a significant reduction in FcαR-mediated ROS production in neutrophils pretreated with anti-LILRA6 compared with IgG1 mAb (Fig. 4D, 4E). Likewise, anti-LILRB3 induced a significantly lower level of FcαR-mediated ROS production compared with IgG2a. Anti-LILRA6 induced a 3.22-fold decrease in FcαR-mediated ROS production compared with IgG1, whereas anti-LILRB3 induced a 1.70-fold decrease in FcαR-mediated ROS production compared with IgG2a. This indicated that LILRB3 could inhibit FcαR-mediated activation and that anti-LILRA6 had a more potent effect than anti-LILRB3.

LILRB3 inhibits FcαR-mediated phagocytosis

The finding that LILRB3 ligation inhibited FcαR-mediated activation suggested that LILRB3 may modulate a broader repertoire of Ab-mediated effector functions. We investigated whether LILRB3 ligation could modulate phagocytic uptake and microbial killing. The ability of LILRB3 to modulate IgA-mediated phagocytosis was tested using IgA1-opsonised microparticles. FITC-labeled DB were coated with HSA and opsonized with anti–HSA-IgA1 or isotype control (Fig. 5A). There was a significant increase in percentage of fluorescent neutrophils incubated with anti–HSA-IgA1 opsonized DB compared with isotype opsonized DB (Fig. 5B, 5C). There was a significant reduction in phagocytic uptake of IgA1-coated DB for neutrophils preincubated on anti-LILRA6 compared with IgG1-coated wells (Fig. 5D, 5E). This indicates LILRB3 stimulation can inhibit FcαR-mediated phagocytosis.

LILRB3 inhibits FcαR-mediated antimicrobial effector functions

As appropriate levels of specific IgA can induce opsonization, phagocytosis, and killing of bacteria (37, 38), we assessed whether LILRB3 ligation can modulate IgA-mediated phagocytosis of live bacteria by neutrophils. Anti–WTA-4497 recognizes β-*O*-GlcNAc modifications on the poly-RboP WTA backbone of *S. aureus* (24, 25, 32). Because *S. aureus* has evolved multiple mechanisms to evade neutrophil phagocytosis and killing (39), we used a *S. capitis* strain manipulated to express poly-RboP WTA with β-*O*-GlcNAc (32). Anti–WTA-4497-IgA1 bound *S. capitis* ATCC 27840-H strain, but

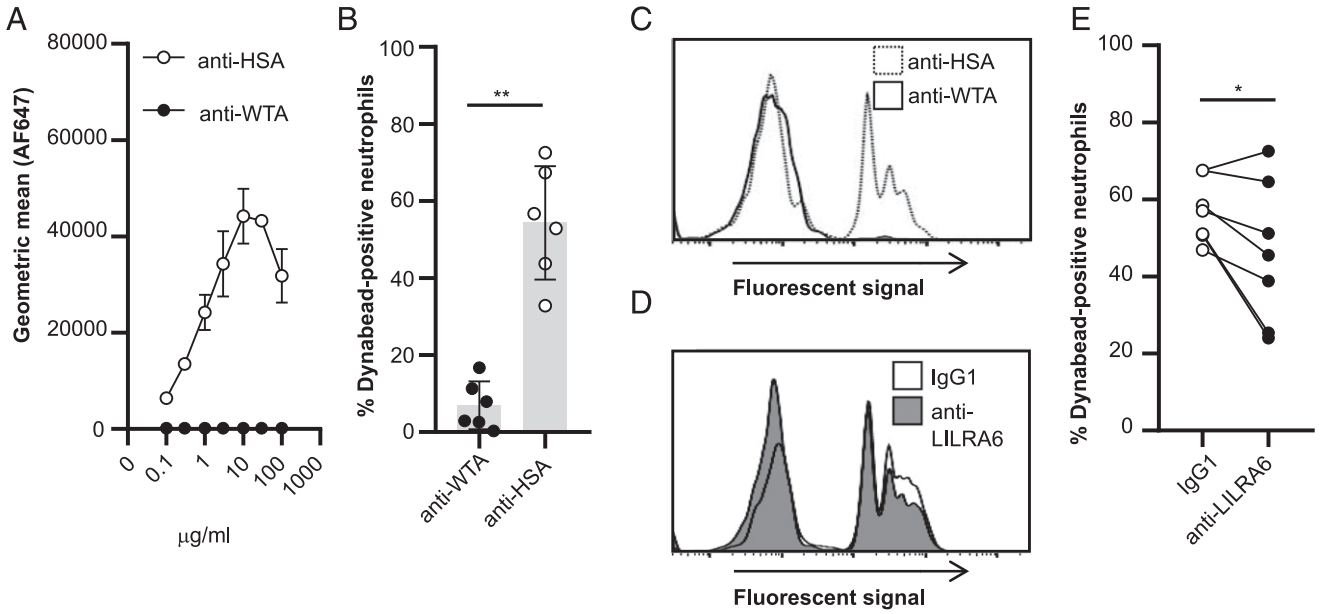

FIGURE 5. LILRB3 inhibits FcαR-mediated phagocytosis. (**A**) Concentration-dependent binding of anti–HSA-IgA1, but not an isotype control to HSA-coated DB ($n = 3$). (**B** and **C**) Phagocytic uptake of IgA-opsonized DB by neutrophils at an MOI of 10:1. Neutrophils were incubated in the presence of 5 μg/ml FLIPr-like for 20 min and then incubated in the presence of IgA1-opsonized FITC-labeled DB for 30 min at 37˚C with 5% CO_2. Fluorescence of neutrophils was measured by flow cytometry analysis. The percentage of fluorescent neutrophils was calculated for each neutrophil population exposed to IgA1-opsonized DB. The integrated results from six separate donors (B) were compared by Student *t* test, and representative flow cytometry plots are shown (C). (**D** and **E**) Continuous ligation of LILRB3 reduces phagocytic uptake of microparticles. Neutrophils were incubated in the presence of 5 μg/ml FLIPr-like for 20 min and then incubated on anti-LILRA6 or IgG1 mAb–coated plates. After 1 h, neutrophils were incubated in the presence of IgA1-opsonized FITC-labeled DB for 30 min at 37˚C with 5% CO_2. A representative experiment (D) and the integrated results from seven separate experiments (E), in which data from the same donor are linked, were compared by Student *t* test. $*p < 0.05$, $**p < 0.01$.

not wild-type strain ATCC 27840 (Fig. 6A, Supplemental Fig. 4E, 4F). There was both IgA1-positive and IgA1-negative ATCC 27840-H populations in repeated experiments (Supplemental Fig. 4E). A total of 55.5% ± 4.17 and 1.83% ± 0.08 ($n = 3$, $p < 0.01$) of the *S. capitis* ATCC 27840-H populations were IgA1 positive when incubated with 3 μg/ml anti–WTA-4497-IgA1 or anti–HSA-IgA1, respectively. The incomplete opsonization of the *S. capitis* population with anti–WTA-4497-IgA1 means there is a proportion of the bacterial population that cannot be phagocytosed through IgA–FcαR interactions. Nonetheless, there was enhanced IgA1 on *S. capitis* ATCC 27840-H bacteria opsonized with anti–WTA-4497-IgA1.

We investigated phagocytosis of FITC-labeled *S. capitis* upon LILRB3 stimulation. A significantly higher proportion of neutrophils were fluorescent when *S. capitis* ATCC 27840-H was opsonized with anti–WTA-4497-IgA1 compared with isotype control (Fig. 6B, 6C). There was a strong trend, although no significant difference, for reduced phagocytic uptake of *S. capitis* during continuous ligation of LILRB3 compared with IgG1 treatment (Fig. 6D, 6E). When normalized for each donor, anti-LILRA6 induced significant reduction in the mean percentage fluorescent neutrophils compared with IgG1 treatment (Fig. 6F).

Finally, we investigated the impact of LILRB3 activation on microbial killing. Neutrophils were infected with *S. capitis* ATCC 27840-H at an MOI of 1 and the number of viable CFU enumerated. Opsonization with anti–WTA-4497-IgA1 led to a significant decrease in the percentage of surviving bacteria compared with anti–HSA-IgA1 opsonization or no opsonization (Fig. 6G). Preincubation of neutrophils on anti-LILRA6–coated wells led to a significant increase in percentage of recovered bacteria compared with IgG1-coated wells (Fig. 6H). There was a 2-fold increase in surviving bacteria when normalizing data for each donor against buffer control–coated wells (Fig. 6I). Our data argue LILRB3 can inhibit IgA-mediated antimicrobial effector functions.

Discussion

Knowledge of inhibitory receptors and paired receptor system properties has considerable implications for disease therapy (5). We aimed to characterize LILRA6 and LILRB3 in neutrophil biology. Our data provide robust evidence that LILRB3 is expressed at a high level on resting neutrophils and that LILRB3 is released in a soluble form upon degranulation. Our data show that LILRB3 is a potent inhibitor of Fc receptor–mediated activation, ROS production, phagocytosis, and microbial killing. The findings broaden our knowledge of the role of LILRB3 in human neutrophil biology.

Our data show high expression of LILRB3 on resting neutrophils. Likewise, other paired receptors such as CEACAM1/3, Siglec-5/14, and SIRPα/β are all expressed at high levels. As anti-LILRA6 and anti-LILRB3 mAb are cross-reactive, it has remained unclear which of these sibling LILRA6 and LILRB3 receptors are expressed by neutrophils. Mass spectrometry analysis provided unequivocal evidence that LILRB3 is expressed on human neutrophils. Additionally, mass spectrometry analysis did not detect any evidence for LILRA6 expression. This suggests LILRA6 expression is not expressed on neutrophils or expression is below detection limits.

Maturation, priming, and activation can reshape the neutrophil surface. We detected no change in LILRB3 surface levels following SV exocytosis, although it is possible that LILRB3-positive SVs were mobilized during neutrophil purification. Our data suggest that priming with TNF-α led to heterogenous LILRB3 surface-expression levels and that activation induces the release of LILRB3 from the surface. Although similar regulation is reported for the inhibitory receptor SIRL-1 (10), this

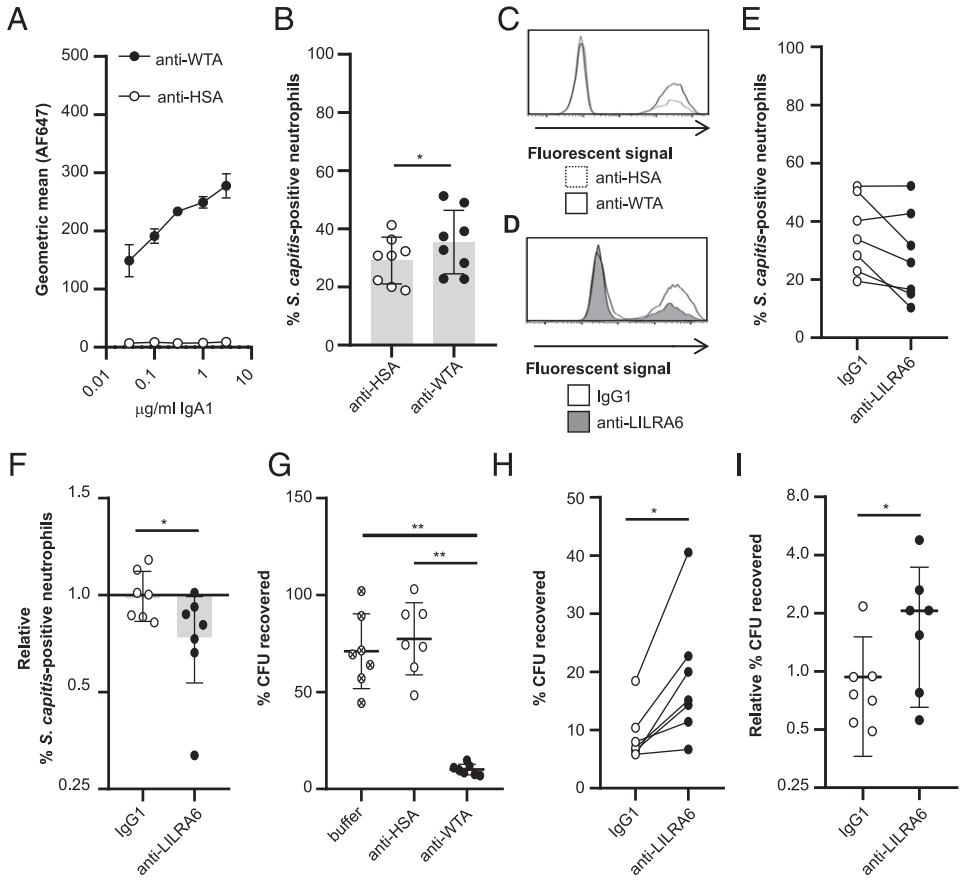

FIGURE 6. LILRB3 suppresses FcαR-mediated antimicrobial effector functions. (**A**) Concentration-dependent binding of anti–WTA-IgA1, but not an isotype control to *S. capitis* ATCC 27840-H strain ($n = 3$). (**B** and **C**) Phagocytic uptake of IgA-opsonized *S. capitis* by neutrophils at an MOI of 10:1. Neutrophils were incubated in the presence of 5 μg/ml FLIPr-like for 20 min and then in the presence of anti-WTA-IgA1–opsonized FITC-labeled *S. capitis* for 30 min at 37˚C with 5% CO_2. Fluorescence of neutrophils was measured by flow cytometry analysis. The percentage of fluorescent neutrophils was calculated for each neutrophil population. The integrated results from eight separate donors (B) were compared by Student *t* test, and representative flow cytometry plots are shown (C). (**D**–**F**) Continuous ligation of LILRB3 reduced phagocytic uptake of *S. capitis* at an MOI of 10:1. Neutrophils were incubated in the presence of 5 μg/ml FLIPr-like for 20 min and then incubated on anti-LILRA6 or IgG1-coated plates. After 1 h, neutrophils were incubated in the presence of anti–WTA-IgA1–opsonized, FITC-labeled *S. capitis* for 30 min at 37˚C with 5% CO_2. Fluorescence of neutrophils was measured by flow cytometry analysis. The percentage of fluorescent neutrophils was calculated for each neutrophil population. A representative experiment (D) and the integrated results from seven separate donors (E), in which data from the same donor are linked, are shown. Relative percentage of fluorescent neutrophils (F) was calculated by normalizing values of against neutrophils preincubated on buffer control–coated wells and was compared by Student *t* test. (**G**) Killing of IgA-opsonized *S. capitis* by neutrophils at an MOI of 1:1. Neutrophils were incubated in the presence of *S. capitis* opsonized with anti–WTA-IgA1 or anti–HSA-IgA or buffer control, for 60 min at 37˚C with 5% CO_2. Following neutrophil lysis, the percentage of CFU recovered at 60 min compared with 0 min was quantified by serial dilution and growth on brain heart infusion agar plates. Data from one donor were removed as an outlier using ROUT method. Data were analyzed by Students *t* test ($n = 7$). (**H** and **I**) Continuous ligation of LILRB3 inhibited bacterial killing. Neutrophils were incubated on anti-LILRA6 or IgG1-coated plates for 1 h prior to incubation for 60 min at 37˚C with 5% CO_2 in the presence of *S. capitis* opsonized with anti–WTA-IgA1 or anti–HSA-IgA or buffer control. After neutrophil lysis, the percentage of CFU recovered at 60 min compared with 0 min was quantified by serial dilution and growth on brain heart infusion agar plates. The integrated results from seven separate donors (H), in which data from the same donor are linked, were compared by Wilcoxon matched-pairs signed-rank test. Relative percentage of recovered CFU (I) was calculated by normalizing values of neutrophils preincubated on anti-LILRA6 or IgG1-coated wells to buffer control and compared Wilcoxon matched-pairs signed-rank test. $*p < 0.05$, $**p < 0.01$.

contrasts other paired receptor systems, including LAIR-1/-2, SIRPα/β, and Siglec-5/14, which are upregulated upon activation (11, 40, 41). Thus, the LILRB3 and SIRL-1 systems are likely to regulate pre- and early-activation functions, whereas LAIR-1/-2, SIRPα/β, and Siglec-5/14 systems may regulate the termination of neutrophil functions. This also contrasts LILRB2, which is upregulated upon degranulation (9).

Modulation of activation thresholds through inhibitory receptors is an important mechanism to control immune cell activity. Our data demonstrate that LILRB3 inhibits IgA-mediated oxidative burst, phagocytosis, and microbial killing in vitro. IgA-opsonized bacteria have previously been shown to be effective at inducing ROS production but less effective at inducing phagocytosis (42). The data from our experiments indicate IgA opsonization had a more profound enhancement on *S. capitis* killing compared with phagocytosis. This suggests that most microbes were killed through release of ROS and antimicrobial molecules. LILRB3 ligation was more effective at inhibiting IgA-induced ROS production than phagocytic uptake in our purified assays. In addition, LILRB3 ligation was more effective at inhibiting killing compared with phagocytosis of IgA-opsonized *S. capitis*. Collectively, this could suggest that IgA-opsonized bacteria are predominately killed through release of ROS and antimicrobial molecules and that LILRB3 is an effective inhibitor of this mechanism.

Our studies used anti-LILR mAb as an agonist. Although our reporter system demonstrated agonistic properties of these mAb against LILRB3, 2B4 NFAT-GFP reporter systems are artificial. Therefore, additional resources need to be developed to identify

agonists that activate LILR-bearing ITIM and ITAM and to improve understanding of signal transduction pathways. In addition, further studies are required with appropriate controls to interrogate signaling mechanisms of LILRB3 in neutrophils.

Bacteria and bacterial products are sensed by phagocytes through pathogen recognition receptors (PRR), including TLRs, GPCRs, and C-type lectin. Upon infection, PRR activation may induce the release of LILRB3 from the surface, allowing ROS production and intracellular killing of microbes at lower activation thresholds. The upregulation of other inhibitory receptors upon activation and degranulation, such as LILRB2, LAIR-1, Siglec-5, and CEACAM1, suggests they contribute to generating balanced immune responses to eliminate bacterial pathogens that do not have damaging effects to tissues.

We focused on investigating modulation of IgA-mediated responses. IgA is the most abundant Ab class at mucosal surfaces and the second most abundant Ab class in serum. Cross-linking FcαR on neutrophils induces a variety of effector functions, including phagocytosis, cytokine release, neutrophil extracellular trap release, and ROS production. LAIR-1 and SIRL-1 have been shown to inhibit FcαR-mediated functions (21, 22). It is tempting to speculate that the LILRB3, LAIR-1, and SIRL-1 systems regulate IgA-mediated responses at mucosal surfaces and serum; although further studies are required. Paired receptor systems are known to regulate FcγR signaling. For example, LILRB1 and LILRB2 modulate FcγR responses on monocytes and/or neutrophils (9, 19). Given that FcαR and certain FcγR (FcγRIa and FcγRIIIa) signal through the Fc receptor common γ-chain, it is likely LILRB3 modulates both IgA- and IgG-mediated responses. However, there is a clear need for investigations to comprehensively assess whether paired receptor systems regulate both IgA- and IgG-mediated functions.

The PLB-985 cell line provides a useful model to study LILRB3 in neutrophil biology, as it possesses functions including ROS production, chemotaxis, and phagocytosis. RNA sequence analysis showed elevated expression of *LILRA6* and *LILRB3* genes during differentiation into neutrophil-like cells (29). We detected a 2.5-fold upregulation in binding of anti-LILRB3 mAb to the surface of PLB-985 cells upon differentiation. Pulldown from DMSO-differentiated PLB-985 lysates detected a single band at 75 kDa in size, which was similar to that identified in pulldown from neutrophils and confirmed as LILRB3. This suggests LILRB3 is expressed in differentiated PLB-985 cells. These data support the hypothesis that LILRB3 functions during neutrophil maturation and/or early-activation phases. The PLB-985 cell system provides a valuable model for improving understanding LILRB3 in neutrophil biology, such as the identification of factors regulating LILRB3 expression and functions.

Identification of LILRB3 ligands is required to further elucidate a role in biology and to provide novel molecular tools. Recently, LILRB3 is reported to bind the complement components C3b, iC3b, C3d, and C4b (43). However, the functional consequences of these interactions remain uncharacterized. LILRB3 has also been shown to interact with a ligand associated with cytokeratin-8 on necrotic glandular epithelial cells (44). However, the specific ligand remains unidentified. LILRB3 could also have ligands and/or functions in a soluble form. This has been demonstrated for other LILR and immune receptors (13, 45).

Bacteria can directly interact with LILRs. This includes *S. aureus*, *Escherichia coli*, and *Helicobacter pylori* that can interact with LILRB3 and LILRB1 (36, 46), and *Mycobacterium* spp. that can interact with LILRA1 and LILRB5. As these bacteria are opportunistic pathogens, it is unclear whether LILRs have evolved as pathogen receptors or whether bacteria have evolved to exploit LILRs. In either scenario, the engagement of LILR by bacteria could have profound impacts on infection outcome.

In summary, the LILRB3 receptor is expressed at a high level on resting neutrophils and can inhibit Fc receptor–mediated functions and microbial killing. Rapid release of soluble LILRB3 upon activation suggests the LILRB3 may provide an important checkpoint to control activation and inflammation during neutrophil maturation. Further studies of LILRB3 inhibition of neutrophil development and functions are warranted. In addition, there is potential for development of immunomodulatory therapeutic approaches by targeting LILRB3.

Acknowledgments

We thank Nina van Sorge (UMC Utrecht) and Matevž Rumpret (UMC Utrecht) for advice and protocols and for providing PLB-985 cells and 2B4 NFAT-GFP T cells and Sjors van der Lans (UMC Utrecht) for technical support.

Disclosures

The authors have no financial conflicts of interest.

References

1. Mócsai, A. 2013. Diverse novel functions of neutrophils in immunity, inflammation, and beyond. *J. Exp. Med.* 210: 1283–1299.
2. Amulic, B., C. Cazalet, G. L. Hayes, K. D. Metzler, and A. Zychlinsky. 2012. Neutrophil function: from mechanisms to disease. *Annu. Rev. Immunol.* 30: 459–489.
3. Futosi, K., S. Fodor, and A. Mócsai. 2013. Neutrophil cell surface receptors and their intracellular signal transduction pathways. *Int. Immunopharmacol.* 17: 638–650.
4. van Rees, D. J., K. Szilagyi, T. W. Kuijpers, H. L. Matlung, and T. K. van den Berg. 2016. Immunoreceptors on neutrophils. *Semin. Immunol.* 28: 94–108.
5. Favier, B. 2016. Regulation of neutrophil functions through inhibitory receptors: an emerging paradigm in health and disease. *Immunol. Rev.* 273: 140–155.
6. Kuroki, K., A. Furukawa, and K. Maenaka. 2012. Molecular recognition of paired receptors in the immune system. *Front. Microbiol.* 3: 429.
7. Steevels, T. A., and L. Meyaard. 2011. Immune inhibitory receptors: essential regulators of phagocyte function. *Eur. J. Immunol.* 41: 575–587.
8. Avril, T., S. D. Freeman, H. Attrill, R. G. Clarke, and P. R. Crocker. 2005. Siglec-5 (CD170) can mediate inhibitory signaling in the absence of immunoreceptor tyrosine-based inhibitory motif phosphorylation. *J. Biol. Chem.* 280: 19843–19851.
9. Baudhuin, J., J. Migraine, V. Faivre, L. Loumagne, A. C. Lukaszewicz, D. Payen, and B. Favier. 2013. Exocytosis acts as a modulator of the ILT4-mediated inhibition of neutrophil functions. *Proc. Natl. Acad. Sci. USA* 110: 17957–17962.
10. Steevels, T. A., R. J. Lebbink, G. H. Westerlaken, P. J. Coffer, and L. Meyaard. 2010. Signal inhibitory receptor on leukocytes-1 is a novel functional inhibitory immune receptor expressed on human phagocytes. *J. Immunol.* 184: 4741–4748.
11. Verbrugge, A., T. de Ruiter, C. Geest, P. J. Coffer, and L. Meyaard. 2006. Differential expression of leukocyte-associated Ig-like receptor-1 during neutrophil differentiation and activation. *J. Leukoc. Biol.* 79: 828–836.
12. Angata, T., T. Hayakawa, M. Yamanaka, A. Varki, and M. Nakamura. 2006. Discovery of Siglec-14, a novel sialic acid receptor undergoing concerted evolution with Siglec-5 in primates. *FASEB J.* 20: 1964–1973.
13. Lebbink, R. J., M. C. van den Berg, T. de Ruiter, N. Raynal, J. A. van Roon, P. J. Lenting, B. Jin, and L. Meyaard. 2008. The soluble leukocyte-associated Ig-like receptor (LAIR)-2 antagonizes the collagen/LAIR-1 inhibitory immune interaction. *J. Immunol.* 180: 1662–1669.
14. Tedla, N., K. Gibson, H. P. McNeil, D. Cosman, L. Borges, and J. P. Arm. 2002. The co-expression of activating and inhibitory leukocyte immunoglobulin-like receptors in rheumatoid synovium. *Am. J. Pathol.* 160: 425–431.
15. Brown, D., J. Trowsdale, and R. Allen. 2004. The LILR family: modulators of innate and adaptive immune pathways in health and disease. *Tissue Antigens* 64: 215–225.
16. Barrow, A. D., and J. Trowsdale. 2008. The extended human leukocyte receptor complex: diverse ways of modulating immune responses. *Immunol. Rev.* 224: 98–123.
17. Hirayasu, K., F. Saito, T. Suenaga, K. Shida, N. Arase, K. Oikawa, T. Yamaoka, H. Murota, H. Chibana, I. Nakagawa, et al. 2016. Microbially cleaved immunoglobulins are sensed by the innate immune receptor LILRA2. *Nat. Microbiol.* 1: 16054.
18. Pereira, S., H. Zhang, T. Takai, and C. A. Lowell. 2004. The inhibitory receptor PIR-B negatively regulates neutrophil and macrophage integrin signaling. *J. Immunol.* 173: 5757–5765.
19. Fanger, N. A., D. Cosman, L. Peterson, S. C. Braddy, C. R. Maliszewski, and L. Borges. 1998. The MHC class I binding proteins LIR-1 and LIR-2 inhibit Fc receptor-mediated signaling in monocytes. *Eur. J. Immunol.* 28: 3423–3434.

20. Lu, H. K., C. Rentero, M. J. Raftery, L. Borges, K. Bryant, and N. Tedla. 2009. Leukocyte Ig-like receptor B4 (LILRB4) is a potent inhibitor of FcgammaRI-mediated monocyte activation via dephosphorylation of multiple kinases. *J. Biol. Chem.* 284: 34839–34848.
21. Steevels, T. A., K. van Avondt, G. H. Westerlaken, F. Stalpers, J. Walk, L. Bont, P. J. Coffer, and L. Meyaard. 2013. Signal inhibitory receptor on leukocytes-1 (SIRL-1) negatively regulates the oxidative burst in human phagocytes. *Eur. J. Immunol.* 43: 1297–1308.
22. Olde Nordkamp, M. J., M. van Eijk, R. T. Urbanus, L. Bont, H. P. Haagsman, and L. Meyaard. 2014. Leukocyte-associated Ig-like receptor-1 is a novel inhibitory receptor for surfactant protein D. *J. Leukoc. Biol.* 96: 105–111.
23. Lubeck, M. D., Z. Steplewski, F. Baglia, M. H. Klein, K. J. Dorrington, and H. Koprowski. 1985. The interaction of murine IgG subclass proteins with human monocyte Fc receptors. *J. Immunol.* 135: 1299–1304.
24. Fong, R., K. Kajihara, M. Chen, I. Hotzel, S. Mariathasan, W. L. W. Hazenbos, and P. J. Lupardus. 2018. Structural investigation of human *S. aureus*-targeting antibodies that bind wall teichoic acid. *MAbs* 10: 979–991.
25. Lehar, S. M., T. Pillow, M. Xu, L. Staben, K. K. Kajihara, R. Vandlen, L. DePalatis, H. Raab, W. L. Hazenbos, J. H. Morisaki, et al. 2015. Novel antibody-antibiotic conjugate eliminates intracellular *S. aureus. Nature* 527: 323–328.
26. Adams, R., L. Griffin, J. E. Compson, M. Jairaj, T. Baker, T. Ceska, S. West, O. Zaccheo, E. Davé, A. D. Lawson, et al. 2016. Extending the half-life of a fab fragment through generation of a humanized anti-human serum albumin Fv domain: an investigation into the correlation between affinity and serum half-life. *MAbs* 8: 1336–1346.
27. Fang, X. T., D. Sehlin, L. Lannfelt, S. Syvänen, and G. Hultqvist. 2017. Efficient and inexpensive transient expression of multispecific multivalent antibodies in Expi293 cells. *Biol. Proced. Online* 19: 11.
28. Stemerding, A. M., J. Köhl, M. K. Pandey, A. Kuipers, J. H. Leusen, P. Boross, M. Nederend, G. Vidarsson, A. Y. Weersink, J. G. van de Winkel, et al. 2013. *Staphylococcus aureus* formyl peptide receptor-like 1 inhibitor (FLIPr) and its homologue FLIPr-like are potent FcγR antagonists that inhibit IgG-mediated effector functions. *J. Immunol.* 191: 353–362.
29. Rincón, E., B. L. Rocha-Gregg, and S. R. Collins. 2018. A map of gene expression in neutrophil-like cell lines. *BMC Genomics* 19: 573.
30. Ohtsuka, M., H. Arase, A. Takeuchi, S. Yamasaki, R. Shiina, T. Suenaga, D. Sakurai, T. Yokosuka, N. Arase, M. Iwashima, et al. 2004. NFAM1, an immunoreceptor tyrosine-based activation motif-bearing molecule that regulates B cell development and signaling. *Proc. Natl. Acad. Sci. USA* 101: 8126–8131.
31. van de Weijer, M. L., M. C. Bassik, R. D. Luteijn, C. M. Voorburg, M. A. Lohuis, E. Kremmer, R. C. Hoeben, E. M. LeProust, S. Chen, H. Hoelen, et al. 2014. A high-coverage shRNA screen identifies TMEM129 as an E3 ligase involved in ER-associated protein degradation. *Nat. Commun.* 5: 3832.
32. Winstel, V., C. Liang, P. Sanchez-Carballo, M. Steglich, M. Munar, B. M. Bröker, J. R. Penadés, U. Nübel, O. Holst, T. Dandekar, et al. 2013. Wall teichoic acid structure governs horizontal gene transfer between major bacterial pathogens. *Nat. Commun.* 4: 2345.
33. Rørvig, S., O. Østergaard, N. H. Heegaard, and N. Borregaard. 2013. Proteome profiling of human neutrophil granule subsets, secretory vesicles, and cell membrane: correlation with transcriptome profiling of neutrophil precursors. *J. Leukoc. Biol.* 94: 711–721.
34. Berger, M., J. O'Shea, A. S. Cross, T. M. Folks, T. M. Chused, E. J. Brown, and M. M. Frank. 1984. Human neutrophils increase expression of C3bi as well as C3b receptors upon activation. *J. Clin. Invest.* 74: 1566–1571.
35. Lebbink, R. J., T. de Ruiter, J. Adelmeijer, A. B. Brenkman, J. M. van Helvoort, M. Koch, R. W. Farndale, T. Lisman, A. Sonnenberg, P. J. Lenting, and L. Meyaard. 2006. Collagens are functional, high affinity ligands for the inhibitory immune receptor LAIR-1. *J. Exp. Med.* 203: 1419–1425.
36. Hogan, L. E., D. C. Jones, and R. L. Allen. 2016. Expression of the innate immune receptor LILRB5 on monocytes is associated with mycobacteria exposure. *Sci. Rep.* 6: 21780.
37. Janoff, E. N., C. Fasching, J. M. Orenstein, J. B. Rubins, N. L. Opstad, and A. P. Dalmasso. 1999. Killing of *Streptococcus pneumoniae* by capsular polysaccharide-specific polymeric IgA, complement, and phagocytes. *J. Clin. Invest.* 104: 1139–1147.
38. Gorter, A., P. S. Hiemstra, P. C. Leijh, M. E. van der Sluys, M. T. van den Barselaar, L. A. van Es, and M. R. Daha. 1987. IgA- and secretory IgA-opsonized *S. aureus* induce a respiratory burst and phagocytosis by polymorphonuclear leucocytes. *Immunology* 61: 303–309.
39. McCarthy, A. J., and J. A. Lindsay. 2013. *Staphylococcus aureus* innate immune evasion is lineage-specific: a bioinfomatics study. *Infect. Genet. Evol.* 19: 7–14.
40. Liu, Y., H. J. Bühring, K. Zen, S. L. Burst, F. J. Schnell, I. R. Williams, and C. A. Parkos. 2002. Signal regulatory protein (SIRPalpha), a cellular ligand for CD47, regulates neutrophil transmigration. *J. Biol. Chem.* 277: 10028–10036.
41. Erickson-Miller, C. L., S. D. Freeman, C. B. Hopson, K. J. D'Alessio, E. I. Fischer, K. K. Kikly, J. A. Abrahamson, S. D. Holmes, and A. G. King. 2003. Characterization of Siglec-5 (CD170) expression and functional activity of anti-Siglec-5 antibodies on human phagocytes. *Exp. Hematol.* 31: 382–388.
42. Vidarsson, G., W. L. van Der Pol, J. M. van Den Elsen, H. Vilé, M. Jansen, J. Duijs, H. C. Morton, E. Boel, M. R. Daha, B. Corthésy, and J. G. van De Winkel. 2001. Activity of human IgG and IgA subclasses in immune defense against *Neisseria meningitidis* serogroup B. *J. Immunol.* 166: 6250–6256.
43. Hofer, J., F. Forster, D. E. Isenman, M. Wahrmann, J. Leitner, M. A. Hölzl, J. J. Kovarik, H. Stockinger, G. A. Böhmig, P. Steinberger, and G. J. Zlabinger. 2016. Ig-like transcript 4 as a cellular receptor for soluble complement fragment C4d. *FASEB J.* 30: 1492–1503.
44. Jones, D. C., C. R. Hewitt, M. R. López-Álvarez, M. Jahnke, A. I. Russell, V. Radjabova, A. R. Trowsdale, and J. Trowsdale. 2016. Allele-specific recognition by LILRB3 and LILRA6 of a cytokeratin 8-associated ligand on necrotic glandular epithelial cells. *Oncotarget* 7: 15618–15631.
45. An, H., V. Chandra, B. Piraino, L. Borges, C. Geczy, H. P. McNeil, K. Bryant, and N. Tedla. 2010. Soluble LILRA3, a potential natural antiinflammatory protein, is increased in patients with rheumatoid arthritis and is tightly regulated by interleukin 10, tumor necrosis factor-alpha, and interferon-gamma. *J. Rheumatol.* 37: 1596–1606.
46. Nakayama, M., D. M. Underhill, T. W. Petersen, B. Li, T. Kitamura, T. Takai, and A. Aderem. 2007. Paired Ig-like receptors bind to bacteria and shape TLR-mediated cytokine production. *J. Immunol.* 178: 4250–4259.